Optoelectronic and Dielectric Properties of Tenorite CuO Thin Films Sprayed at Various Molar Concentrations

Ouarda Ben Messaoud[1], Abdelouahab Ouahab[1*], Saâd Rahmane[1], Souheila Hettal[1], Aicha Kater[1], Moustefa Sayad[1,2], Hafida Attouche[1], Noureddine Gherraf[3]

[1] Laboratory of Physics of Thin Films and Applications, Mohamed Khider University, P. O. B. 145 RP, 07000 Biskra, Algeria
[2] Laboratory of New and Renewable Energies in Arid and Saharan Zones, University of Kasdi Merbah Ouargla, P. O. B. 511, 30 000 Ouargla, Algeria
[3] Laboratory of Natural Resources and Management of Sensitive Environments, University Larbi Ben M'hidi Oum El Bouaghi, P. O. B. 358, 04000 Oum El Bouaghi, Algeria
* Corresponding author, e-mail: a.ouahab@univ-biskra.dz

Abstract

The work in hand presents the elaboration of CuO thin films using a home-made spray pyrolysis technique at room atmosphere. The films were synthesized on preheated glass substrate at 450 °C. The source solution molarity was varied from 0.025 to 0.1 mol/L. The films were characterized by employing X-Ray Diffraction technique, UV-Vis-NIR spectrophotometry, Scanning Electron Microscope imagery, Energy Dispersive Spectroscopy, and four-points probe techniques. The X-ray diffraction analysis confirmed that all films are polycrystalline with a preferred orientation along the plane (−111) of the monoclinic crystal structure phase of tenorite (CuO). The SEM images showed a homogeneous and smooth surface. Crystallinity and grain size were improved. The rise of solution concentration induced a reduction of transmittance and reflectance in the visible region. The energy gap, the absorption coefficient, the extinction coefficient, refractive index, dielectric constant (ε_r and ε_i) and loss energy were estimated from transmittance and reflectance data. The gap energy decreases from 2.72 to 2.56 eV. The film deposited for 0.025 mol/L exhibits the highest real part of the dielectric constant ($\varepsilon_r \sim 17$). The film resistivity which is in order of 10^2 Ω cm decreases with the increase of molar concentration. The estimated dielectric constant indicated that the resulting CuO thin films could be used as dielectric layers for optoelectronic devices working in Vis-NIR region of radiation. Furthermore, the relatively high band gap, high absorption coefficient and high conductivity of the film obtained at 0.075 mol/L, make them good candidates as absorption layers in solar cells applications.

Keywords

copper oxide, spray pyrolysis, dielectric constant, molarity, opto-electronic

1 Introduction

In recent years, researchers are focusing their attention on metal oxide semiconductors for numerous material science applications, including optoelectronic, photovoltaic, and magnetic systems [1]. Copper oxide thin films have sparked a great deal of interest among transition metal oxides due to their *p-type* semiconducting [2]. The two most frequent stable forms of copper oxides are tenorite (CuO) and cuprite (Cu_2O) which have a monoclinic and cubic crystal structure respectively. Both of them are *p-type* semiconductor due to the Cu^{2+} vacancies in the structure [3]. However, CuO, which is a low-cost material, abundant in nature, non-toxic, and with a good chemical stability, exhibits a high solar absorbance, a narrow band gap (1.21–1.9 eV) [3], and a low thermal emittance [4]. It is also known by its good electrical and optical properties such as dielectric constant and refractive index of 18.1 and 1.4 respectively [5], and an absorption coefficient as high as 10^5 cm^{-1} [3]. Owing to its advantages, copper oxide has attracted attention for different technological areas such as gas sensors [6], photo-catalysis [7], lithium batteries [8], solar cells [9], supercapacitors [10], optoelectronic devices [11] etc. Several chemical and physical manufacturing methods for CuO thin films are reported in the literature such as chemical bath deposition [12], sol-gel [13], SILAR [4], pulsed laser deposition [14], sputtering [5], spray pyrolysis [6, 15] and electro-deposition [16].

Spray pyrolysis can produce good quality CuO thin films, besides its simplicity and less material consumption.

Based on the previous studies [6, 17–19], the investigation of optoelectronic properties especially the dielectric function of Tenorite is too few. Herein, in this paper, copper oxide thin layers were synthesized on glass substrate by spray pyrolysis technique (SPT). CuO thin films structural, morphological, and optical properties were investigated with varying the source solution molar concentration. A special focus on the refractive index (n), extinction coefficient (k), real part (ε_r) and imaginary part (ε_i) of dielectric constants is given and the obtained results are discussed.

2 Experimental details
2.1 Materials and CuO thin films deposition
Tenorite copper oxide (CuO) thin films were deposited by a home-made spray pyrolysis experimental setup [20] at 450 °C. Glass microscope slides (25 mm × 19 mm × 12 mm) were used as a substrate cleaned previously by immersion in acetone (from VWR CHEMICALS prolabo with purity 99.5%), ethanol (from VWR CHEMICALS prolabo with purity of 96.3%) and distilled water for 10 min before drying. The source solutions with different concentrations (0.025, 0.05, 0.075, and 0.1 mol/L) were prepared by dissolving appropriate masses of copper chloride dehydrate precursor ($CuCl_2$-$2H_2O$) (from BIOCHEM Chemopharma with purity of 97%) each in 50 mL of distilled water and stirred magnetically to obtain a homogeneous blue solution. Then, the aqueous solutions were sprayed by compressor air gas in fine droplets from atomizer perpendicularly onto the preheated substrate. The deposition time, nozzle –substrate distance, pressure and flow rate were kept constant during deposition at 3 min, 30 cm, 1 bar and 5 mL/min respectively. At the end of deposition, the substrates were left on the hot plate to cool slowly to room temperature to avoid their fracture and damage due to heat shock.

2.2 Characterization techniques
The crystalline properties of CuO thin layer were characterized by XRD technique using Rigaku-Type MiniFlex600 diffractometer with Cu Kα radiation (λ = 1.5418 Å) operated at 40 kV and 30 mA. A JASCO V-770 spectrophotometer was used to record the thin film optical transmittance and reflectance in the wavelength range of 380–1500 nm. Chemical composition and surface morphology of the obtained films were determined by two associated devices Energy Dispersive Spectroscopy (EDS) and TESCAN

VEGA3 SEM. Finally, the electrical data (resistivity) was obtained by means of a KEITHLEY 2400 SourceMeter four-point probe measurements.

3 Results and discussion
3.1 Thickness growth and films formation
When the droplets of aqueous solution were felt on the hot substrate surface, CuO was formed thermally by thermal decomposition of hydrated copper chloride and water. The sprayed copper chloride atomized solution thermally reacted on the hot sample surface according to Eq. (1):

$$CuCl_2 + H_2O \rightarrow CuO(s) + 2HCl(g) . \tag{1}$$

Uniform, black color and adherent (hardly peeled with scotch tape test) thin films were obtained. Films thicknesses (d) were measured by weight deference method using the following formula [21]:

$$d = \frac{m}{gA} \tag{2}$$

where m is the mass of film obtained using a 10^{-4} g sensitive balance, g is the density of deposited film, and A is its surface area.

For comparison purpose, the thickness of the sample deposited at 0.05 mol/L was measured using SEM cross section; the obtained value (160 nm) was very close to that obtained was the weight deference method (174 nm) used for all samples with an estimation error of 8%. Fig. 1 shows the variation of thickness with the increase of molar concentration. The thickness of the film increased simply due to the increased amount of the deposited material by increasing molar concentration. The thickness may be
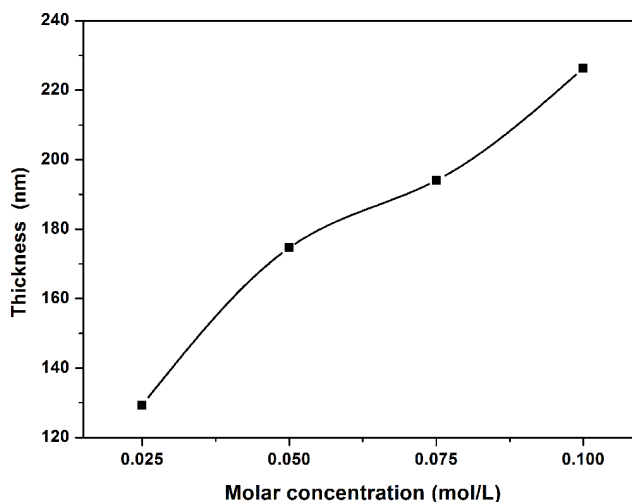

Fig. 1 Thickness variation of CuO thin films as a function of molar concentration

governed by Cu-containing species. It is difficult to control the insertion of O^{2-} into the film during the growth process using the spray pyrolysis technique.

3.2 Structural properties

The XRD patterns of CuO thin films produced at different molar concentrations are assembled and shown in Fig. 2. It can be seen that all samples have polycrystalline structure. The diffraction of X-rays shows peaks at $2\theta = 35.6°$, 38.8°, and 53.5° corresponding to (−111), (111), (020) reticular planes respectively. Low intensity reflection peaks (110) and (220) appearing at 32.57° and 68.13° were identified. The deposited thin films have tenorite (CuO) phase and monoclinic structure with the space group C2/c according to JCPDS (No. 00-041-0254). In contrast to our results, Moumen et al. [22] found that the films obtained at a molar concentration of 0.035 mol/L were amorphous. Moreover, according to the literature, pure tenorite (CuO) phase has been obtained by Al Ghamdi et al. [17] and Akaltun [4]. No diffraction peaks indicate other phases of copper oxides Cu_2O and/or Cu_3O_4 were found in any of the thin films.
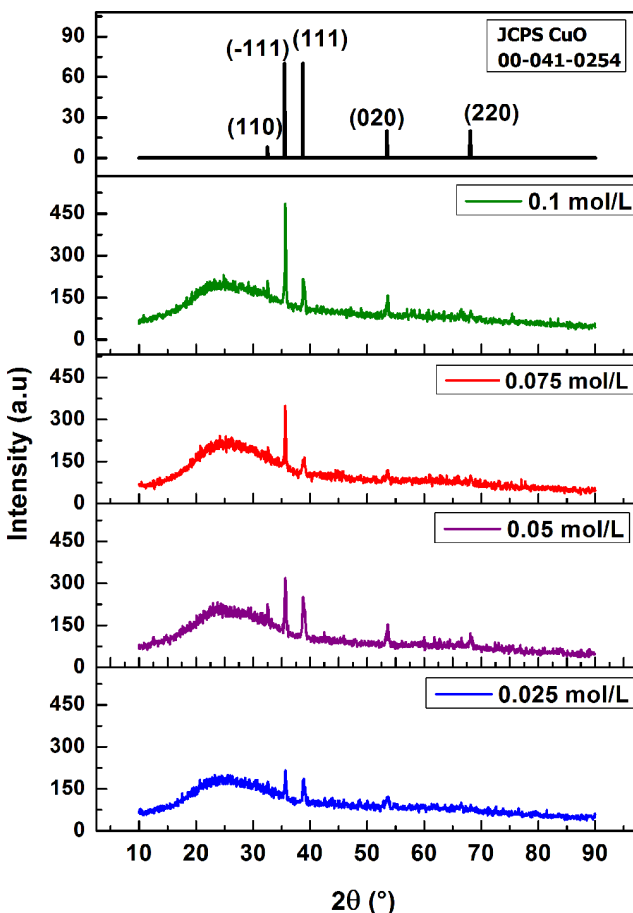

Fig. 2 XRD patterns of copper oxide CuO depending on precursor concentrations

The films have the same intense peak according to the plan (−111) which was the preferred orientation. It indicated that there are more particles aligned in this plane. Similar result was found by Hettal et al. [23]. Roy and Bhuiyan [24] who obtained sprayed thin films with preferential (111) planes using cupric acetate as solution source. In the same context, Prakash et al. [18] got two major peaks, (−111) and (111) at the same molarity values respectively. It's clear from Fig. 2 the concentration 0.025 mol/L has poor crystallinity, and by increasing molar concentration, the intensity of the peak (−111) increases. This probably due to the enhancement in grain growth following the arrival of droplets with more concentrated reactive material, consequently improving the films crystallinity.

The average crystallite size is estimated by Debye–Sherrer formula [25]:

$$D = \frac{0.9\lambda}{\beta \cos\theta} \tag{3}$$

where D is the crystallite size (nm), λ the X-ray wavelength (1.5418 Å), θ the Bragg diffraction angle (in radian). The β is the full-width-at-half-maximum (FWHM). The strain ε and the dislocation density δ values are calculated using by Eq. (4) and Eq. (5) [25]:

$$\varepsilon = \beta \frac{\cos\theta}{4} \tag{4}$$

and

$$\delta = \frac{1}{D^2} . \tag{5}$$

By applying Eq. (6), and Eq. (7) on XRD data of the peaks we found the lattice constants (a, b and c), for the monoclinic phase structure, which obey the expressions:

$$2d_{hkl} \sin\theta_{hkl} = n\lambda \tag{6}$$

and

$$\frac{1}{d_{hkl}^2} = \frac{1}{\sin^2\beta}\left[\frac{h^2}{a^2} + \frac{k^2 \sin^2\beta}{b^2} - \frac{2hk\cos\beta}{ac}\right] \tag{7}$$

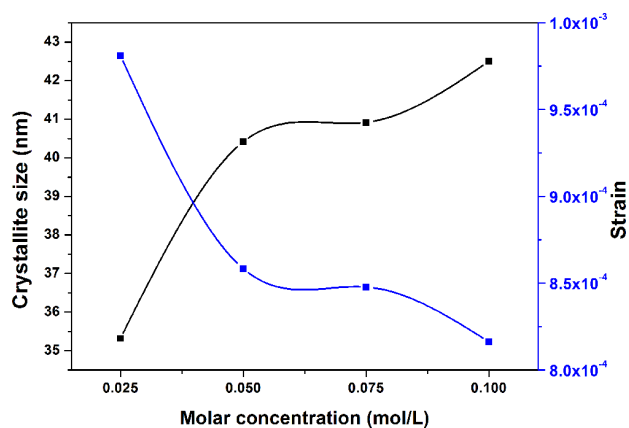where d_{hkl} and (hkl) are the inter-planer distance and Miller indices. The values of Bragg angle (2θ), inter-planar distance (d_{hkl}), crystallite size, strain, and the dislocation and lattice parameters are listed in Table 1. The reported lattice constant values are close to the related standard JCPDS card values ($a_0 = 4.685$, $b_0 = 3.423$, $c_0 = 5.132$ Å, $\alpha = \gamma = 90°$ and $\beta = 99.52°$ is the angle between a and c lattice vectors), and no changes are observed, which suggests

Table 1 Structural and lattice parameters of CuO thin layer as function of molar concentration

Molar concentration (mol/L)	2θ (°)	hkl	d_{hkl} (Å)	D (nm)	ε (10^{-4})	δ $(10^{10}$ $1/cm^2)$	Lattice constant (Å)
0.025	35.683	(−111)	2.516	35.319	9.811	8.016	$a = 4.675$ $b = 3.413$ $c = 5.253$
0.05	35.596	(−111)	2.521	40.416	8.583	6.122	$a = 4.680$ $b = 3.421$ $c = 5.126$
0.075	35.643	(−111)	2.518	40.917	8.478	5.973	$a = 4.681$ $b = 3.425$ $c = 5.013$
0.1	35.651	(−111)	2.518	56.581	6.131	3.124	$a = 4.689$ $b = 3.420$ $c = 5.1517$

the absence of any other phases like Cu_2O or Cu_4O_3. It was also observed that the calculated values of the inter-planar distance (d_{hkl} = 2.524 Å) were found to be lower than the standard value and the predominant peak moves to the right to the standard peak position (2θ = 35.539°) which indicates that the crystallites undergo a compressive stress.

Fig. 3 represents the crystallite size and strain variations as a function of precursor solutions concentration. The crystallite size increases from 35 to 56 nm with the increase of molar concentration from 0.025 to 0.1 mol/L due to coalescence of grains. Similar results are reported by Dhas et al. [19]. Abdelmounaïm et al. [6] observed that the crystallite size of copper oxide films increased from 0.05 to 0.2 mol/L. Smaller values of 4 to 6 nm were obtained by spray pyrolysis for substrate temperature of 350 °C [26]. Whereas the strain values were reduced from 9.81 × 10⁻⁴ to 6.13 × 10⁻⁴ depending on precursor molarities. As the solution concentration increases, more Cu and O atoms in the surface substrate are precipitated and they experience more interactions which contributes to an enlargement of the crystallites and leads to bigger grains and subsequently

Fig. 3 Crystallite size and strain variations with molar concentration

the enhancement of film's crystallinity [27]. Furthermore, the lattice defects along the grain boundaries are reduced due to the increase of crystallites size, which may lead to decreasing strain and dislocation densities [28], as seen in Table 1. The minimum values of δ and strain ε are found to be 3.1 × 10¹⁰ line/cm² and 6.13 × 10⁻⁴ respectively at solution molarity of 0.1 mol/L. These observations indicate the good crystallinity in the films of CuO.

3.3 Optical properties
3.3.1 Transmittance, reflectance, absorption coefficient, optical energy band gap and Urbach energy

The optical transmittance (T) and reflectance (R) of our sprayed copper oxide (tenorite) thin films were measured using UV-VIS-NIR Spectrometer in the wavelength range from 380 to 1500 nm. These spectra were used to extract optical parameters and quality of CuO thin films. Fig. 4 (a) represents the transmittance data for CuO thin films by the effect of molar concentration of spray solution. The films were found to be highly absorbing in the visible region and transparent in near-infrared region with an average transmittance range of 70 to 80%. Also, all samples behaved as opaque material below 500 nm. Indeed, the transmittance decreases in visible range when the precursor solution increases to 0.075 mol/L due to the absorption of light as a result to the excitation of electrons from the valence band to the conduction band of CuO which is a *p*-type semiconductor. These spectra are similar to those of copper oxide films deposited using spray pyrolysis as reported in [12, 26, 29]. Furthermore, the absorption edge is shifted toward the longer wavelength side (redshift). This result demonstrates a reduction in the energy band gap of films. Consequently, the reduction in the film transparency can be attributed to the rise of the density of atoms which leads
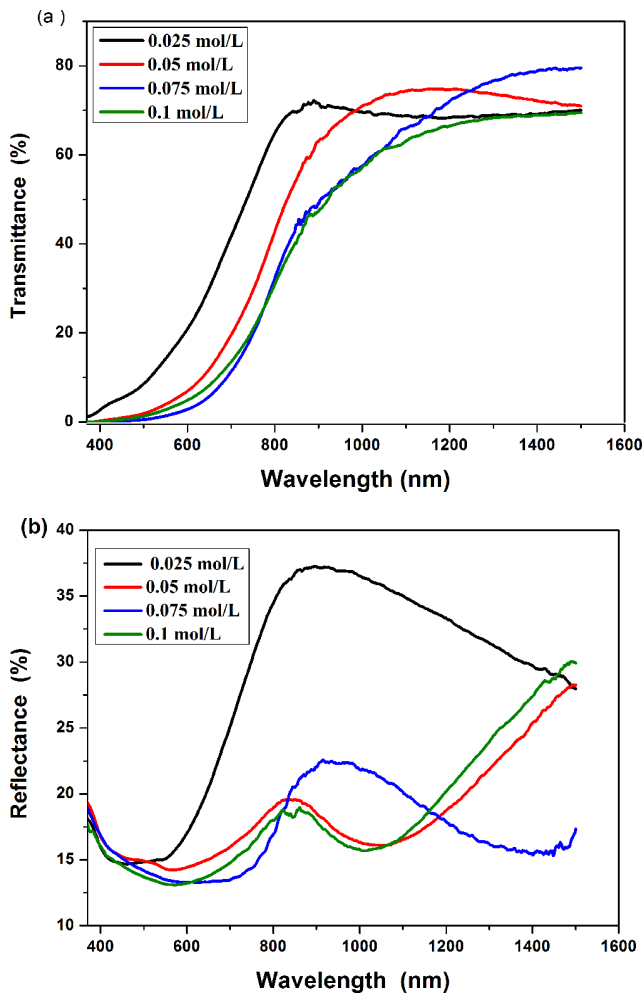
Fig. 4 (a) Optical transmittance and (b) reflectance spectra of copper oxide thin films as function of wavelengths with different molar concentrations

due to the film porosity which in turn reduces light scattering [33] and allowing additional light to pass through. This observation is confirmed by the morphological results.

The optical reflectance spectra of CuO thin films, which provide information about scattered light from the surface of films upon molar concentrations, is shown in Fig. 4 (b). It can be noted from the graphs that the reflectivity of the thin films at all molarities have the same pathway. It decreases below 400 nm, then increases with increasing wavelengths in visible range (500–800 nm) and then it decreases in the NIR range. The average reflectance is less than 40% for wavelengths in the 380 to 1500 nm domain. This agrees very well with Mugwang'a et al. [34] who observed low values of reflectance below 45% for copper oxide thin films. On the other hand, as a precursor solution increases, the reflection of film decreases due to the rise of film thickness [35]. Hussein and Al-Mayalee [36] and Singh and Kaur [37] have obtained the same behavior. Furthermore, our films exhibit low reflectance in the visible spectrum. This shows high absorbance when compared to the transmittance spectrum which makes copper oxide a good absorber material for solar cells applications [34]. The optical parameters such as absorption coefficient, band gap, extinction coefficient, refractive index and dielectric constant are determined from optical transmittance and reflectance spectra. The value of absorption coefficient of thin film is calculated using by Eq. (8) [38]:

$$\alpha = \frac{1}{d} \ln \frac{1-R}{T} \qquad (8)$$

where α is the absorption coefficient, d the film thickness, T the transmittance, and R the reflectance. Fig. 5 (a) shows the variations of the absorption coefficient of the studied films. All the films have absorption coefficient α superior to 10^5 cm^{-1} in the visible range, which agrees with the

to the optical scattering phenomenon at the grain boundaries [30, 31] and the grain growth of CuO films [32]. Another reason for the decline in transmission is the higher film absorption associated with larger film thickness [31], which is easily evident from the appearance of the black color. Nevertheless, the increase of T for sample 0.1 mol/L
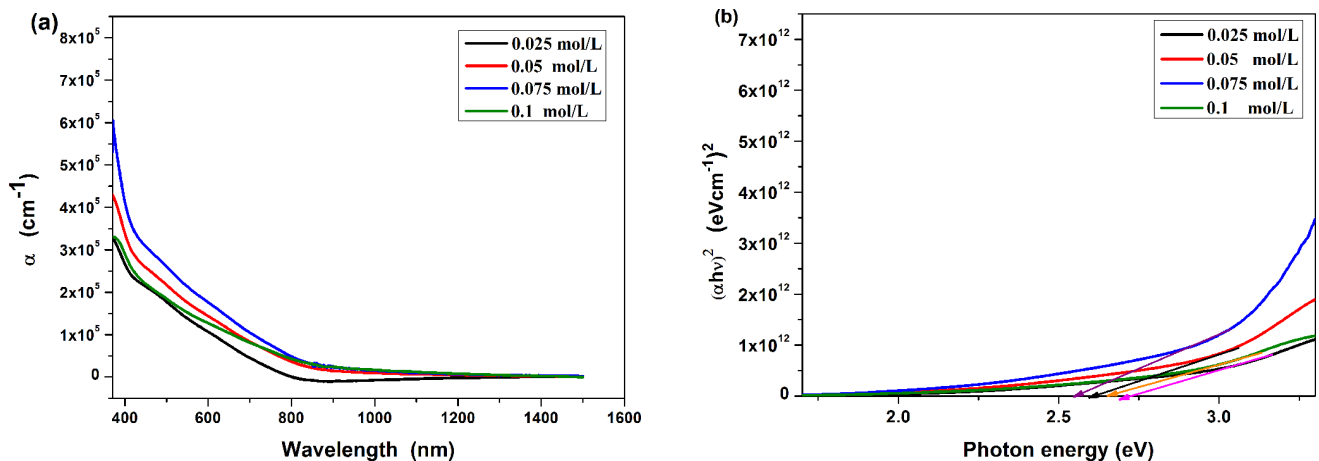

Fig. 5 (a) Optical absorption coefficient and (b) Tauc plots spectra for CuO thin film deposited with different molarities

reported results in the literature [9]. For the NIR region of the light spectrum, it is clear that α is almost vanishing to zero. It is always suggested to use a high optical absorption coefficient in thin-film solar cell applications as an absorber layer. It is also noted that the absorption coefficient increases with increasing copper concentrations, especially at 0.075 mol/L then decreases at 0.1 mol/L. The reduction in α with the wavelength indicates that the layer became more transparent which agrees with transmittance results.

In order to determine the energy band gap of films, the material has direct band gap, we plot $(\alpha h v)^2$ versus $(h v)$, by using the Tauc formula [39]:

$$\left(\alpha h v\right)^2 = B\left(h v - E_g\right) \tag{9}$$

where $h v$ is the incident photon energy and B is a constant. The E_g is obtained by extrapolation of the plot of $(\alpha h v)^2$ as a function of $h v$, as shown in Fig. 5 (b). The Urbach energy (E_u) (band tail width), is the disorder in film. It is calculated from the inverse of the slope of $\log(\alpha)$ versus $(h v)$ according to Eq. (10) [39]:

$$\alpha = \alpha_0 e^{\frac{h v}{E_u}} \tag{10}$$

where α_0 is a constant. The obtained band gap energy and band tail width values at different molar concentrations are summarized in Table 2. It is noted that on increasing the precursor solution concentration up to 0.075 mol/L, the band gap was reduced from 2.72 to 2.56 eV, then it was risen to 2.64 eV at molarity 0.1 mol/L. Similar behavior of the narrowing in band gap energy upon the increased molarity solution was reported on metal oxide by Attouche et al. [40] and Barir et al. [41]. The drop in E_g is consistent with the absorption edge to red shift described above in Fig. 4 (a). It can be also explained by the increase in band tail width as shown in Table 2, which may have resulted from the appearance of structural defects in the film due to its preparation conditions; this could lead to the allowed states close to the conduction band in the forbidden region. These allowed states may merge with the conduction band with the increasing solution concentration,

resulting in a reduction in the band gap [25]. Besides, the rise of Cu concentration (shift of stoichiometry in favor of copper) contributes to the creation of donor states within the energy gap close to the conductive band, hence the Fermi level is shifted toward the conduction band. On the other hand, the improvement in crystalline quality of the films as the growth of bigger crystallites which is confirmed by XRD may be another reason for decreasing band gap energy [13]. In contrast, the widening effect on the band gap can be related to the decrease in band tail width, since E_u values change inversely with band gap energy as shown in Table 2. Lower disorder incomes in less defect states present in the films. These E_g values are higher than those given in the references [13, 19, 20]. Bhowmik et al. [42], and Prakash et al. [18] found that for copper oxide films produced by sol-gel and spray pyrolysis technique E_g varied between 1.47 and 1.27 eV, and 1.5 and 2.03 eV versus precursor concentration respectively. Similar observations were found for films sprayed at 350 °C from copper acetate monohydrate solutions of different high molarities (0.1–0.2 mol/L) which reported the reducing of band gap from 2.55 to 2.5 eV [9]. Other researchers reported large band gap compared to the bulk oxide [23].

3.3.2 Extinction coefficient and refractive index

It should be noted that understanding the optical dielectric constant and thin-film refractive index is crucial for creating any special optical device. The refractive index is closely related to the concepts of polarization ability of atoms when they are subject to an electric field inside the materials [43]. The mathematical equation of the complex refractive index (n^*) of thin films is given by Eq. (11):

$$n^* = n + ik . \tag{11}$$

The imaginary part (the extinction coefficient k) indicates the amount of light scattering and absorption in the medium per unit volume, and the real part (the refractive index, n) gives information about the refraction of light. The following equations are used to calculate the extinction coefficient and refractive index respectively [43]

Table 2 Optical parameters and resistivity of CuO thin layers versus precursor solutions
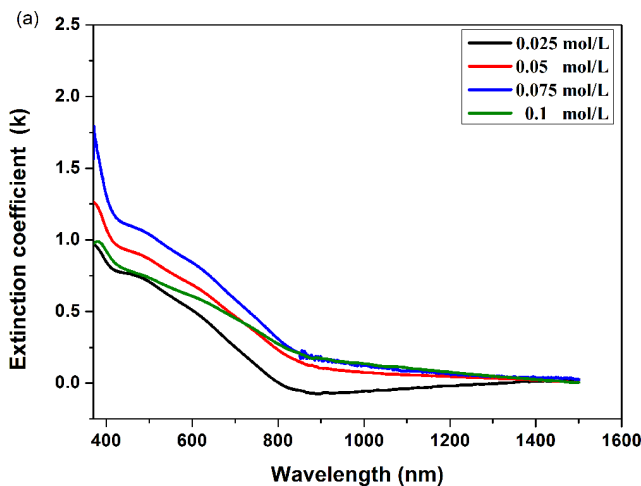
Molar concentration (mol/L)	E_g (ev)	E_u (ev)	k	n	ε_r	ε_i	R_{sheet} (Ω)	ρ (Ω cm)
0.025	2.72	0.29	0.123	3.428	11.77	0.847	3.17×10^7	4.10×10^2
0.05	2.60	0.35	0.352	2.361	5.45	1.663	1.54×10^7	2.68×10^2
0.075	2.56	0.63	0.452	2.144	4.47	1.894	6.59×10^6	1.27×10^2
0.1	2.64	0.44	0.367	2.276	5.05	1.672	4.73×10^6	1.07×10^2

R_{sheet}: sheet resistance

$$k = \frac{\alpha \lambda}{4\pi} \qquad (12)$$

$$n = \frac{1+R}{1-R} + \sqrt{\frac{4R}{(1-R)^2} - k^2} \,. \qquad (13)$$

The variation of k and n versus wavelength at various molarities are plotted in Fig. 6 (a) and (b). We note that the extinction coefficient decreases with an increase in the wavelength. The loss due to scattering and absorbance decreases with an increase in wavelength [44]. The k value was found to range between 0.94 and 1.78 for visible wavelength domain ($\lambda <$ 800 nm), whereas it was close to zero in the near infrared region ($\lambda >$ 800 nm), which indicated the transparency of the films [45]. The same behavior was observed for semiconducting Fe_2O_3 [45] thin films. Otherwise, the extinction coefficient tends to increase when precursor concentration increased. The low value of k suggests that the thin film has good surface smoothness. On the other hand, Fig. 6 (b) shows an increase in the refractive index for wavelengths lower than 900 nm; known as the abnormal dispersion, then it decreases continuously for longer wavelengths which represents the normal dispersion behavior. The $n(\lambda)$ reaches higher values in the range 8 to 4.14 for the sample prepared using 0.025 mol/L molar concentration. Such high refractive index films are appropriate for anti-reflection coatings. As the source solution molarity increases, the refractive index reduces from 3.8 to 2.38 due to increase of thickness. The curve change seems to have the same behavior as the reflection spectrum. Similar observation was found by Roy and Bhuiyan [24] where n value decreases from 2.82 to 2.52 for 0.05 to 0.1 mol/L. This decrease could also be a result of the increase in particle size [42]. The effects

due to the crystallite size which is in the order of 35 nm and the possibility of the presence of voids which increases the scattering of light through the thin film. With the increase of grains agglomeration, a decrease in refractive index, and this is confirmed by the previous results. The evolution of n and k with increasing of solutions molarity at $\lambda =$ 750 nm (taken as reference for comparison) in Table 2. Prakash et al. [18], Chala et al. [38] found that the refractive index n rises as the molarity increased for CuO and ZnO thin films. Our n value was higher than those found by Prakash et al. [18] which ranged between 2.83 and 2.9.

3.3.3 Optical dielectric constant

The study of material's dielectric properties is important for various electronic device technologies since it is correlated to their ability to obstruct electron transit when polarized by an external electric field [46]. The complex dielectric constant is given by Eq. (14):

$$\varepsilon^* = \varepsilon_r + i\varepsilon_i \,. \qquad (14)$$

Generally, the real and imaginary parts of dielectric constants are evaluated from the values of k and n using Eq. (15) and Eq. (16) [43]:

$$\varepsilon_r = n^2 - k^2 \qquad (15)$$

$$\varepsilon_i = 2nk \,. \qquad (16)$$

Fig. 7 (a) and (b) illustrate the real and imaginary parts of optical dielectric constant of CuO films as a function of molar concentration. The real part represents the stored energy, and the imaginary part represents the loss in the material [47]. From Fig. 7 (a) and (b), we note that ε_r and ε_i values varied from 1 to 17 and from 0.03 to 3.5
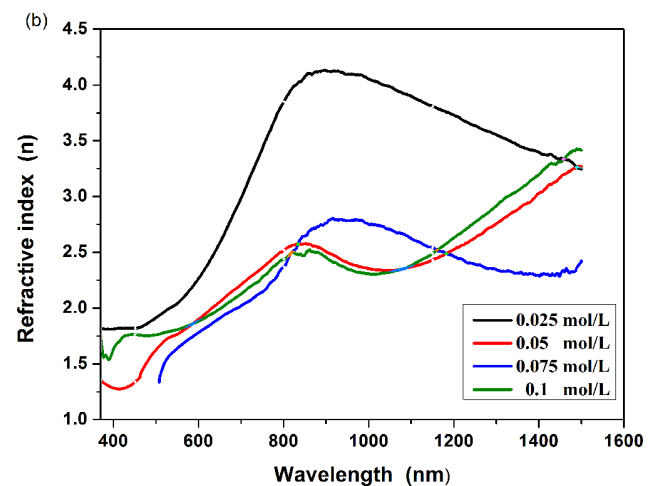

Fig. 6 (a) Extinction coefficient (k) and (b) refractive index (n) of CuO thin film versus precursor solution concentration
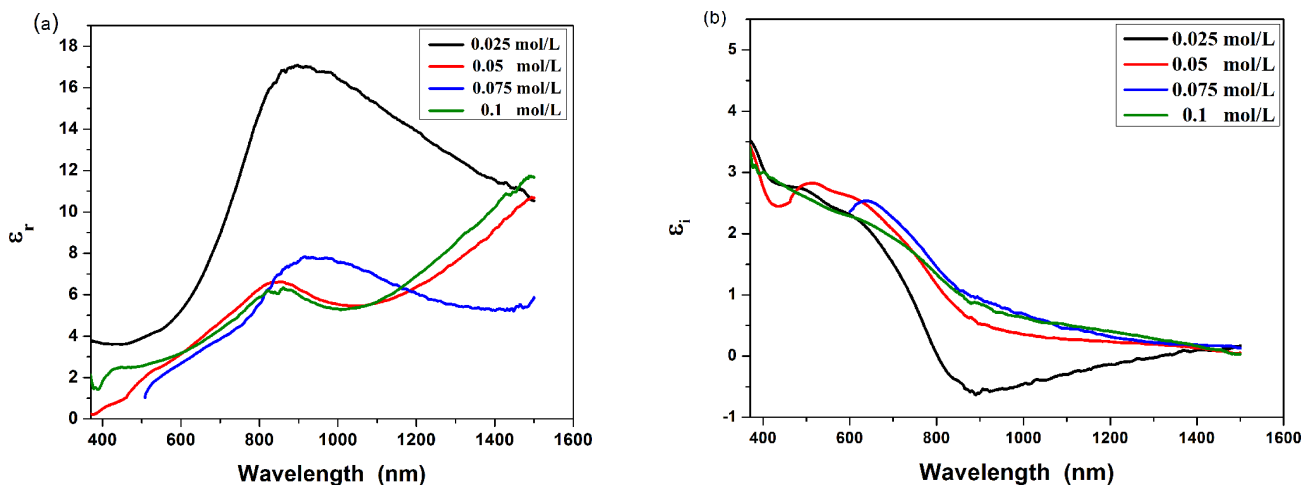
Fig. 7 (a) The real (ε_r) and (b) imaginary (ε_i) parts of the dielectric constant of the CuO thin film versus precursor solution concentration

as a function of wavelength respectively. The real part is higher than the imaginary part which indicates a weak energy loss of light within the film [48]. This effect can be explained by a larger crystallites size, which results in fewer grain boundaries, which reduces optical losses [48]. This proves the good quality of the film growth, and thus enhancing their optical properties making these layers suitable for optoelectronic applications [49]. Furthermore, ε_r value decreases along with the rise of ε_i as the molarity of solution increases until 0.075 mol/L, then increases again at 0.1 mol/L, respectively.

Both real and imaginary part of complex dielectric constant exhibit similar behavior of *n* and *k* because of the close relationship between them as demonstrated in Eq. (15) and Eq. (16). The maximum value of ε_r was obtained using a lower concentration of the source solution (0.025 mol/L). The values of ε_r and ε_i for various molar concentration at $\lambda = 750$ nm are tabulated in Table 2. Earlier, it was reported that the dilute precursor solution improves the dielectric response of thin films due to the crystallite size modification, lower porosity and change in preferred orientation [50].

In a dissipative system, the factor tanδ is related to the rate of power loss [43]. Dielectric loss tangent is given in the following formula:

$$\tan \delta = \frac{\varepsilon_i}{\varepsilon_r} . \qquad (17)$$

The relation between tanδ and the wavelength for the films is seen in Fig. 8. As we can see, tanδ rises as the wavelength increases.
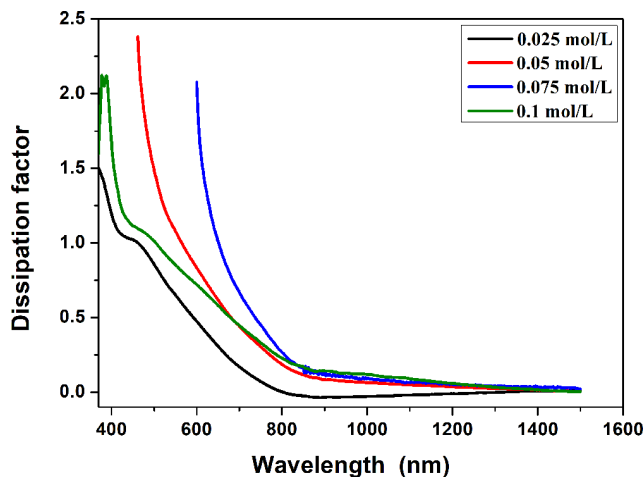

Fig. 8 Dielectric loss tangent of CuO thin films

3.4 Morphological properties

The surface morphology of the sprayed CuO films were analyzed by scanning electron microscopy (SEM) at 10.000× magnification. SEM images of these films coated at different molar concentrations of copper source solution are shown in Fig. 9. We note that all the films are well covered, smooth and uniform deposited on the glass substrates without any cracks. Also, they are well adhered to the substrate. It can be clearly seen from Fig. 9 that for low molar concentration, there is a difference in the distribution, the shape of grains and their sizes demonstrating the presence of several crystallographic orientations according basically to the planes (111) and (−111) confirmed by XRD analysis as seen in the related previous section. As the concentration of the solution increases, the distribution and the size of grain become more homogenous and uniform. This observation indicated that the
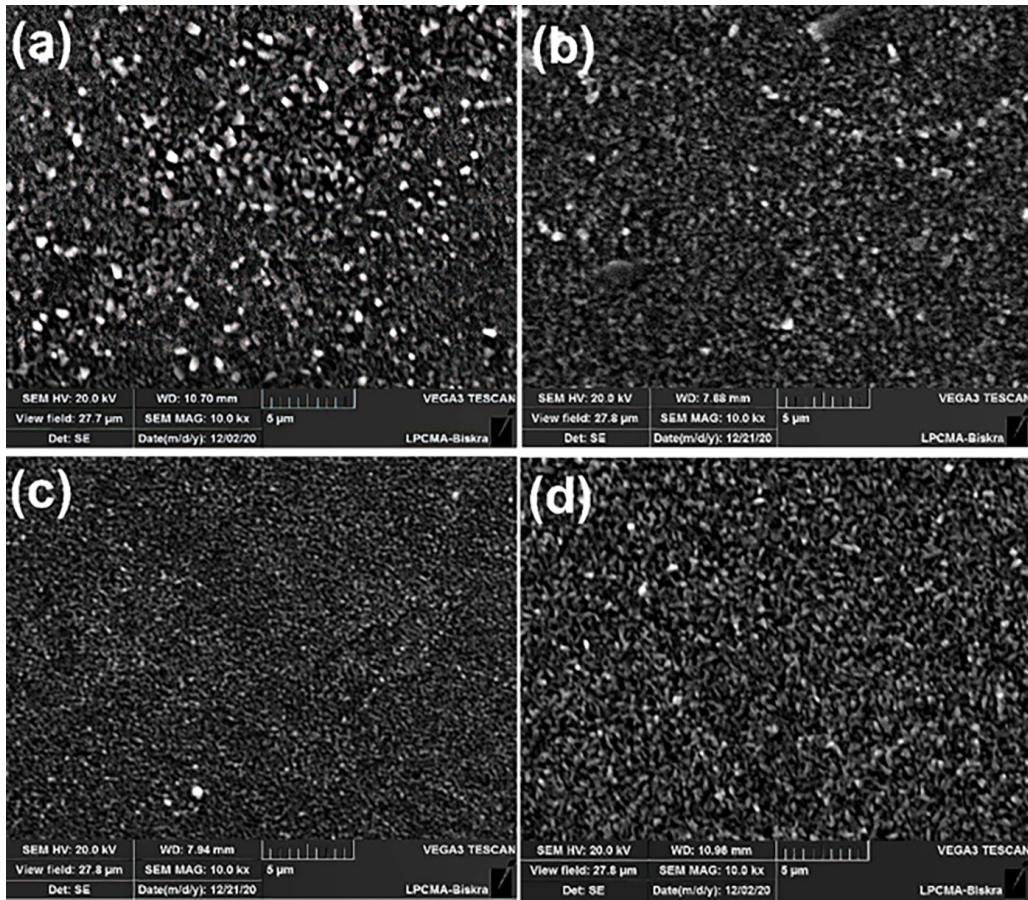
Fig. 9 SEM micrographs of copper oxide thin films that were prepared at (a) 0.025 mol/L, (b) 0.05 mol/L, (c) 0.075 mol/L and (d) 0.1 mol/L

grains grow according to the same orientation (−111). It's also noteworthy that the crystallite size increases when the molarity of solution varies from 0.025 to 0.1 mol/L. It can be seen also from Fig. 9 (d) that the surface of the deposited film at 0.1 mol/L is compact and rough. Further, it had large grain size compared with the other molarities. This result indicates that the higher concentration of solute particles leads to more agglomeration of crystalline grains hence, improving the crystallinity of material. Fig. 10 shows the EDS spectra of the prepared films at 0.1 mol/L.
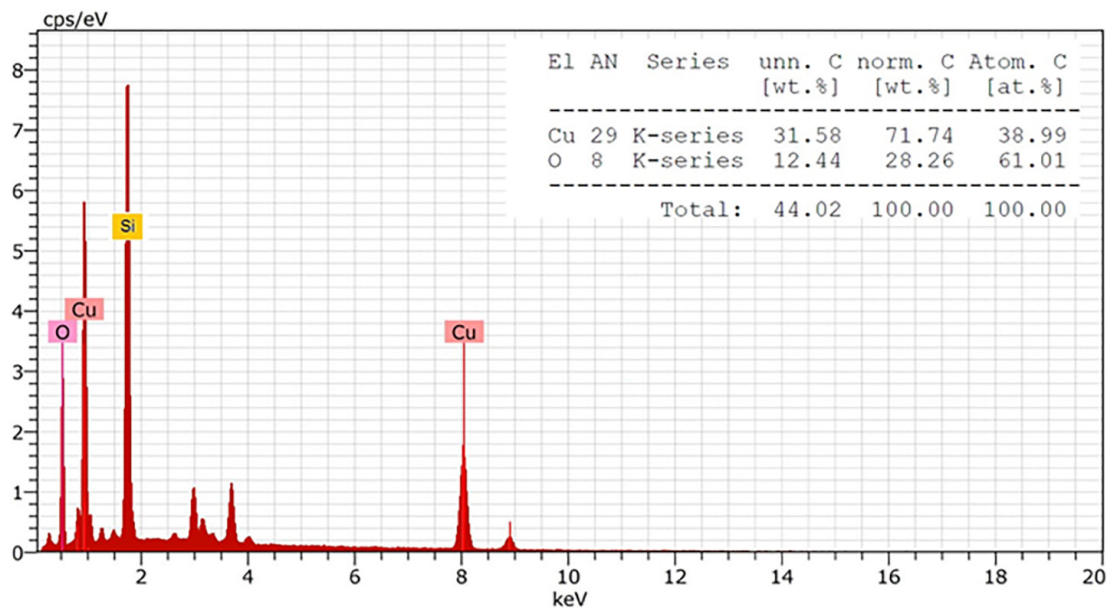

Fig. 10 EDS spectrum of CuO film deposited from 0.1 mol/L concentration

It confirms the presence of elemental composition Cu and O in the deposited film in addition to Si which comes from the glass substrate. The atomic fraction of Cu and O are 38.99% and 61.01% respectively.

3.5 Electrical properties

Electrical properties were analyzed by the four-point probe measurement system at room temperature to determine the film resistivity using the formula below:

$$\rho = dR_{\text{sheet}} = d\pi \frac{V}{I \ln 2} \tag{18}$$

where R_{sheet} is the sheet resistance, ρ is the resistivity, d is the film thickness, I is the applied current and V is the resulting voltage.

The resistivity of thin films versus molar concentration represented in Fig. 11. It is clear that, as the precursor concentration rises from 0.025 to 0.1 mol/L; the resistivity of copper oxide thin films drops from 4.10×10^2 to 1.07×10^2 (Ω cm). It is known that CuO has p-type conductivity due to presence of cation vacancy and is related to the positive carrier density (holes). This decrease of ρ can be explained by the elevation of free carrier concentration (holes) as the film thickness increases [51]. The increase of hole concentration is due either to the rise of the vacancy concentration of cations or to the increase in interstitial oxygen. Both cases enhance the shift of film stoichiometry from its normal value. On the other hand, the high conductivity can be ascribed to the films' increased crystallinity. The increase of crystallite size with increase in the precursor mola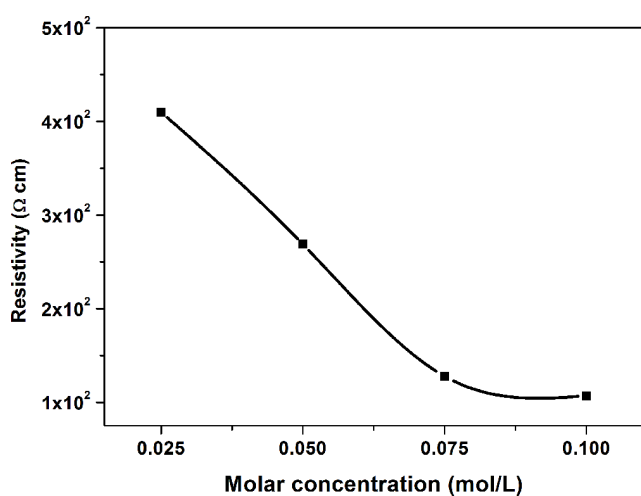rity leads to a reduction of the trapping states at grain boundaries, and hence, the carrier mobility rises [40] as a consequence the conductivity increases. Otherwise, the resistivity and real part of dielectric constant have the same behavior, both are reducing as represent in Table 2.

4 Conclusion

Polycrystalline copper oxide CuO thin films were grown on glass substrates at 450 °C using a simple spray pyrolysis apparatus. The effect of the different solution concentrations ranging between 0.025 and 0.1 mol/L on the surface morphology, structural, optics, and electric properties have been studied. Scanning electron microscopy (SEM) shows that all films are well covered, have good homogeneity and adherence to the substrate and no cracks could be detected. The EDX analysis confirms the presence of copper and oxygen elements. The structural analysis revealed the polycrystalline nature of CuO films with monoclinic structures. The mean grain size increases from ~35 to ~56 nm as the molarity rises from 0.025 to 0.1 mol/L. Subsequently, the transmission and reflection spectrum decreased in the visible range whereas the absorption coefficient increases ($\alpha \geq 10^5$ 1/cm) owing to the reduction of band gap from 2.72 to 2.56 eV with the rise of source solution molarity. The extinction coefficient k and the refractive index n were found in the range 0.9–1.76 and 2.38–3.8 respectively. The films prepared for low concentration have the best real part of dielectric constant value ~17. In contrast, low value of the imaginary part of constant permittivity and loss energy were found as the molarity is reduced from 0.1 to 0.025 mol/L. The resistivity decreased down to its minimum value of 107 Ω cm for 0.1 mol/L source concentration. In one hand, the films obtained at 0.075 mol/L are good candidate as absorption layer in solar cells applications since they have good electrical conductivity, and high absorption coefficient in the UV-VIS-IR range, and in the other hand, the samples obtained at 0.025 mol/L have good dielectric constant which makes them suitable for optoelectronic applications such as NIR-VIS detection.

Fig. 11 Electrical resistivity variations of CuO thin films as a function of precursor molar concentration

References

[1] Özmenteş, R. "Characterization of cupric oxide thin films prepared by nebulizer spray technique", Materials Today: Proceedings, 46, pp. 6916–6919, 2021.
https://doi.org/10.1016/j.matpr.2021.01.558

[2] Parvathy, T., Muhammed Sabeer, N. A., Mohan, N., Pradyumnan, P. P. "Effect of dopant gas pressure on the growth of magnetron sputtered CuO thin films for electrical and optical applications", Optical Materials, 125, 112031, 2022.
https://doi.org/10.1016/j.optmat.2022.112031

[3] Naveena, D., Logu, T., Dhanabal, R., Sethuraman, K., Bose, A. C. "Comparative study of effective photoabsorber CuO thin films prepared via different precursors using chemical spray pyrolysis for solar cell application", Journal of Materials Science: Materials in Electronics, 30(1), pp. 561–572, 2019.
https://doi.org/10.1007/s10854-018-0322-4

[4] Akaltun, Y. "Effect of thickness on the structural and optical properties of CuO thin films grown by successive ionic layer adsorption and reaction", Thin Solid Films, 594, pp. 30–34, 2015.
https://doi.org/10.1016/j.tsf.2015.10.003

[5] Tombak, A., Benhaliliba, M., Ocak, Y. S., Kiliçoglu, T. "The novel transparent sputtered p-type CuO thin films and Ag/p-CuO/n-Si Schottky diode applications", Results in Physics, 5, pp. 314–321, 2015.
https://doi.org/10.1016/j.rinp.2015.11.001

[6] Abdelmounaïm, C., Amara, Z., Maha, A., Mustapha, D. "Effects of molarity on structural, optical, morphological and CO_2 gas sensing properties of nanostructured copper oxide films deposited by spray pyrolysis", Materials Science in Semiconductor Processing, 43, pp. 214–221, 2016.
https://doi.org/10.1016/j.mssp.2015.12.019

[7] Liu, J., Jin, J., Deng, Z., Huang, S. Z., Hu, Z. Y., Wang, L. Wang, C., Chen, L.H., Li, Y., Van Tendeloo, G., Su, B. L. "Tailoring CuO nanostructures for enhanced photocatalytic property", Journal of Colloid and Interface Science, 384(1), pp. 1–9, 2012.
https://doi.org/10.1016/j.jcis.2012.06.044

[8] Pang, H., Deng, J., Yan, B., Ma, Y., Li, G., Ai, Y., Chen, G., Zhang, J., Zheng, H., Du, J. "Cupric Oxide Nanorods on Double-Face Copper Micropuzzles Electrode as Promising Anode Materials for Lithium ion batteries", [pdf] International Journal of Electrochemical Science, 7(11), pp. 10735–10747, 2012. Available at: http://www.electrochemsci.org/papers/vol7/71110735.pdf [Accessed: 27 February 2023]

[9] Shabu, R., Moses Ezhil Raj, A., Sanjeeviraja, C., Ravidhas, C. "Assessment of CuO thin films for its suitablity as window absorbing layer in solar cell fabrications", Materials Research Bulletin, 68, pp. 1–8, 2015.
https://doi.org/10.1016/j.materresbull.2015.03.016

[10] Krishnamoorthy, K., Kim, S.-J. "Growth, characterization and electrochemical properties of hierarchical CuO nanostructures for supercapacitor applications", Materials Research Bulletin, 48(9), pp. 3136–3139, 2013.
https://doi.org/10.1016/j.materresbull.2013.04.082

[11] Yu, X., Marks, T. J., Facchetti, A. "Metal oxides for optoelectronic applications", Nature Materials, 15(4), pp. 383–396, 2016.
https://doi.org/10.1038/nmat4599

[12] Ramya, V., Neyvasagam, K., Chandramohan, R., Valanarasu, S., Benial, A. M. F. "Studies on chemical bath deposited CuO thin films for solar cells application", Journal of Materials Science: Materials in Electronics, 26(11), pp. 8489–8496, 2015.
https://doi.org/10.1007/s10854-015-3520-3

[13] Shariffudin, S. S., Khalid, S. S., Sahat, N. M., Sarah, M. S. P., Hashim, H. "Preparation and Characterization of Nanostructured CuO Thin Films using Sol-gel Dip Coating", IOP Conference Series: Materials Science and Engineering, 99(1), 012007, 2015.
https://doi.org/10.1088/1757-899X/99/1/012007

[14] Faiz, H., Siraj, K., Khan, M. F., Irshad, M., Majeed, S., Rafique, M. S., Naseem, S. "Microstructural and optical properties of dysprosium doped copper oxide thin films fabricated by pulsed laser deposition technique", Journal of Materials Science: Materials in Electronics, 27(8), pp. 8197–8205, 2016.
https://doi.org/10.1007/s10854-016-4824-7

[15] Fasasi, A. Y., Osagie, E., Pelemo, D., Obiajunwa, E., Ajenifuja, E., Ajao, J., Osinkolu, G., Makinde, W. O., Adeoye, A. E. "Effect of Precursor Solvents on the Optical Properties of Copper Oxide Thin Films Deposited Using Spray Pyrolysis for Optoelectronic Applications", American Journal of Materials Synthesis and Processing, 3(2), pp. 12–20, 2018.
https://doi.org/10.11648/j.ajmsp.20180302.12

[16] Rahal, H., Kihal, R., Affoune, A. M., Rahal, S. "Effect of Solution pH on Properties of Cuprous Oxide Thin Films Prepared by Electrodeposition from a New Bath", Journal of Electronic Materials, 49(7), pp. 4385–4391, 2020.
https://doi.org/10.1007/s11664-020-08093-y

[17] Al Ghamdi, S. D., Alzahrani, A. O. M., Aida, M. S., Abdel-wahab, M. S. "Influence of substrate temperature and solution molarity on CuO thin films' properties prepared by spray pyrolysis", Journal of Materials Science: Materials in Electronics, 33(18), pp. 14702–14710, 2022.
https://doi.org/10.1007/s10854-022-08390-8

[18] Prakash, A., V. S., G. K., Moger, S. N., Mahesha, M. G. "Spectroscopic and electrical analysis of spray deposited copper oxide thin films", Materials Today Communications, 32, 103926, 2022.
https://doi.org/10.1016/j.mtcomm.2022.103926

[19] Dhas, C. R., Alexander, D., Christy, A. J., Jeyadheepan, K., Raj, A. M. E., Raja, C. J. "Preparation and Characterization of CuO Thin Films Prepared by Spray Pyrolysis Technique for Ethanol Gas Sensing Application", Asian Journal of Applied Sciences, 7(8), pp. 671–684, 2014.
https://doi.org/10.3923/ajaps.2014.671.684

[20] Abdelkrim, A., Rahmane, S., Abdelouahab, O., Abdelmalek, N., Brahim, G. "Effect of solution concentration on the structural, optical and electrical properties of SnO_2 thin films prepared by spray pyrolysis", Optik, 127(5), pp. 2653–2658, 2016.
https://doi.org/10.1016/j.ijleo.2015.11.232

[21] Abdelkrim, A., Rahmane, S., Nabila, K., Hafida, A., Abdelouahab, O. "Polycrystalline SnO_2 thin films grown at different substrate temperature by pneumatic spray", Journal of Materials Science: Materials in Electronics, 28(6), pp. 4772–4779, 2017.
https://doi.org/10.1007/s10854-016-6122-9

[22] Moumen, A., Hartiti, B., Thevenin, P., Siadat, M. "Synthesis and characterization of CuO thin films grown by chemical spray pyrolysis", Optical and Quantum Electronics, 49(2), 70, 2017.
https://doi.org/10.1007/s11082-017-0910-1

[23] Hettal, S., Ouahab, A., Rahmane, S., Benmessaoud, O., Kater, A., Sayad, M. "Effect of the Number of Dips on the Properties of Copper Oxide Thin Films Deposited by Sol-Gel Dip-Coating Technique", Iranian Journal of Materials Science and Engineering, 19(1), pp. 1–8, 2022.
https://doi.org/10.22068/ijmse.2582

[24] Roy, S. S., Bhuiyan, A. H. "Properties of Spray Pyrolysied Copper Oxide Thin Films", [pdf] Sensors & Transducers, 209(2), pp. 20–27, 2017. Avaiable at: https://www.sensorsportal.com/HTML/DIGEST/february_2017/Vol_209/P_2899.pdf [Accessed: 27 February 2023]

[25] Abdelkrim, A., Rahmane, S., Abdelouahab, O., Hafida, A., Nabila, K. "Optoelectronic properties of SnO_2 thin films sprayed at different deposition times", Chinese Physics B, 25(4), 046801, 2016.
https://doi.org/10.1088/1674-1056/25/4/046801

[26] Daira, R., Kabir, A., Boudjema, B., Sedrati, C. "Structural and optical transmittance analysis of CuO thin films deposited by the spray pyrolysis method", Solid State Sciences, 104, 106254, 2020.
https://doi.org/10.1016/j.solidstatesciences.2020.106254

[27] Xu, L., Zheng, G., Miao, J., Xian, F. "Dependence of structural and optical properties of sol–gel derived ZnO thin films on sol concentration", Applied Surface Science, 258(19), pp. 7760–7765, 2012.
https://doi.org/10.1016/j.apsusc.2012.04.137

[28] Sarma, M. P., Wary, G. "Effect of Molarity on Structural and Optical Properties of Chemically Deposited Nanocrystalline PbS Thin Film", International Letters of Chemistry, Physics and Astronomy, 74, pp. 22–35, 2017.
https://doi.org/10.18052/www.scipress.com/ilcpa.74.22

[29] Al-Ghamdi, A. A., Khedr, M. H., Shahnawaze Ansari, M., Hasan, P. M. Z., Abdel-Wahab, M. S., Farghali, A. A. "RF sputtered CuO thin films: Structural, optical and photo-catalytic behavior", Physica E: Low-dimensional Systems and Nanostructures, 81, pp. 83–90, 2016.
https://doi.org/10.1016/j.physe.2016.03.004

[30] Rodríguez-Báez, J., Maldonado, A., Torres-Delgado, G., Castanedo-Pérez, R., Olvera, M. D. L. L. "Influence of the molar concentration and substrate temperature on fluorine-doped zinc oxide thin films chemically sprayed", Materials Letters, 60(13–14), pp. 1594–1598, 2006.
https://doi.org/10.1016/j.matlet.2005.11.077

[31] Dhas, C. R., Venkatesh, R., Sivakumar, R., Raj, A. M. E., Sanjeeviraja, C. "Effect of solution molarity on optical dispersion energy parameters and electrochromic performance of Co_3O_4 films", Optical Materials, 72, pp. 717–729, 2017.
https://doi.org/10.1016/j.optmat.2017.07.026

[32] Vignesh, R., Sivakumar, R., Sanjeeviraja, C. "A detailed analysis on optical parameters of spinel structured Mn_3O_4 thin films deposited by nebulized spray pyrolysis technique", Optical Materials, 111, 110580, 2021.
https://doi.org/10.1016/j.optmat.2020.110580

[33] Gençyılmaz, O., Taşköprü, T., Atay, F., Akyüz, İ. "Synthesis, characterization and ellipsometric study of ultrasonically sprayed Co_3O_4 films", Applied Physics A, 121(1), pp. 245–254, 2015.
https://doi.org/10.1007/s00339-015-9417-4

[34] Mugwang'a, F. K., Karimi, P. K., Njoroge, W. K., Omayio, O., Waita, S. M. "Optical characterization of Copper Oxide thin films prepared by reactive dc magnetron sputtering for solar cell applications", International Journal of Thin Films Science and Technology, 2(1), pp. 15–24, 2013. [online] Available at: https://digitalcommons.aaru.edu.jo/cgi/viewcontent.cgi?article=1096&context=ijtfst [Accessed: 27 February 2023]

[35] Gahtar, A., Benramache, S., Ammari, A., Boukhachem, A., Ziouche, A. "Effect of molar concentration on the physical properties of NiS thin film prepared by spray pyrolysis method for supercapacitors", Inorganic and Nano-Metal Chemistry, 52(1), pp. 112–121, 2022.
https://doi.org/10.1080/24701556.2020.1862225

[36] Hussein, H. A., Al-Mayalee, K. H. "Study the Effect of Thickness on the Optical Properties of Copper Oxide Thin Films by FDTD Method", Turkish Journal of Computer and Mathematics Education (TURKOMAT), 12(12), pp. 3865–3870, 2021. [online] Available at: https://www.turcomat.org/index.php/turkbilmat/article/view/8172 [Accessed: 27 February 2023]

[37] Singh, P., Kaur, D. "Influence of film thickness on texture and electrical and optical properties of room temperature deposited nanocrystalline V_2O_5 thin films", Journal of Applied Physics, 103(4), 043507, 2008.
https://doi.org/10.1063/1.2844438

[38] Chala, S., Bdirina, M., Elbar, M., Naoui, Y., Benbouzid, Y. Taouririt, T. E., Labed, M., Boumaraf, R., Bouhdjar, A. F., Sengouga, S., Yakuphanoğlu, F., Rahmane, S. "Dependence of Structural and Optical Properties of ZnO Thin Films Grown by Sol-Gel Spin-Coating Technique on Solution Molarity", Transactions on Electrical and Electronic Materials, 23(5), pp. 544–551, 2022.
https://doi.org/10.1007/s42341-022-00386-9

[39] Rahmane, S., Djouadi, M. A., Aida, M. S., Barreau, N. "Oxygen effect in radio frequency magnetron sputtered aluminium doped zinc oxide films", Thin Solid Films, 562, pp. 70–74, 2014.
https://doi.org/10.1016/j.tsf.2014.03.073

[40] Attouche, H., Rahmane, S., Hettal, S., Kouidri, N. "Precursor nature and molarities effect on the optical, structural, morphological, and electrical properties of TiO_2 thin films deposited by spray pyrolysis", Optik, 203, 163985, 2020.
https://doi.org/10.1016/j.ijleo.2019.163985

[41] Barir, R., Benhaoua, B., Benhamida, S., Rahal, A., Sahraoui, T., Gheriani, R. "Effect of Precursor Concentration on Structural Optical and Electrical Properties of NiO Thin Films Prepared by Spray Pyrolysis", Journal of Nanomaterials, 2017, 5204639, 2017.
https://doi.org/10.1155/2017/5204639

[42] Bhowmik, D. R., Ahmed, A. N., Gafur, M. A., Miah, M. Y., Islam, D. "Effect of Process Variables on Deposited Cupric Oxide Thin Film by Sol-Gel Spin Coating Technique", IOP Conference Series: Materials Science and Engineering, 438(1), 012001, 2018.
https://doi.org/10.1088/1757-899X/438/1/012001

[43] Vignesh, R., Sivakumar, R., Sanjeeviraja, C. "Phase tuning of nebulized spray deposited manganese oxide thin films by the effect of annealing temperature and their linear and non-linear optical parameters", Optik, 254, 168687, 2022.
https://doi.org/10.1016/j.ijleo.2022.168687

[44] Aparna, C., Mahesha, M. G., Kumara Shetty, P. "Structural and optical properties of indium oxide thin films synthesized at different deposition parameters by spray pyrolysis", Materials Today: Proceedings, 55, pp. 141–147, 2022.
https://doi.org/10.1016/j.matpr.2022.01.048

[45] Ben Ayed, R., Ajili, M., Turki, N. K. "Physical properties and Rietveld analysis of Fe_2O_3 thin films prepared by spray pyrolysis: Effect of precursor concentration", Physica B: Condensed Matter, 563, pp. 30–35, 2019.
https://doi.org/10.1016/j.physb.2019.03.029

[46] El-Damhogi, D. G., ELesh, E., Ibrahim, A. H., Mosaad, S., Makhlouf, M. M., Mohamed, Z. "The impact of radiation on the morphological, structural properties, linear and nonlinear optical parameters of gallium phthalocyanine chloride thin films for optoelectronic devices", Radiation Physics and Chemistry, 195, 110060, 2022.
https://doi.org/10.1016/j.radphyschem.2022.110060

[47] Farea, A. M. M., Kumar, S., Batoo, K. M., Yousef, A., Lee, C. G., Alimuddin "Structure and electrical properties of $Co_{0.5}Cd_xFe_{2.5-x}O_4$ ferrites", Journal of Alloys and Compounds, 464(1–2), pp. 361–369, 2008.
https://doi.org/10.1016/j.jallcom.2007.09.126

[48] Nefzi, C., Souli, M., Cuminal, Y., Kamoun-Turki, N. "Effect of sulfur concentration on structural, optical and electrical properties of Cu_2FeSnS_4 thin films for solar cells and photocatalysis applications", Superlattices and Microstructures, 124, pp. 17–29, 2018.
https://doi.org/10.1016/j.spmi.2018.09.033

[49] Nagaraja, B. S., Gurumurthy, S. C., Bairy, R., Ramam, K., Bindu, K., Rao, A. "A systematic investigation on structural, electrical, linear and nonlinear optical properties of Zn:CdO thin films for optoelectronic applications", Optical Materials, 122, 111669, 2021.
https://doi.org/10.1016/j.optmat.2021.111669

[50] Yahia, A., Attaf, A., Saidi, H., Dahnoun, M., Khelifi, C., Bouhdjer, A., Saadi, A., Ezzaouia, H. "Structural, optical, morphological and electrical properties of indium oxide thin films prepared by sol gel spin coating process", Surfaces and Interfaces, 14, pp. 158–165, 2019.
https://doi.org/10.1016/j.surfin.2018.12.012

[51] Kouidri, N., Rahmane, S. "Effect of Cobalt Chloride Concentration on Structural, Optical and Electrical Properties of Co_3O_4 Thin Films Deposited by Pneumatic Spray", Journal of New Technology and Materials, 10(1), pp. 56–62, 2020.
https://doi.org/10.12816/0058152